

# Investigation into the Solid-Solution $(\text{Na}_{1-x}\text{K}_x)_2\text{Mo}_2\text{O}_7$ Ceramic and the Effect on Sintering Property

X. Yuan<sup>\*1, 3</sup>, H. Liu<sup>1</sup>, Y. Wei<sup>2</sup>, Y. Wang<sup>1</sup>, Q. Gao<sup>1</sup>

<sup>1</sup>*School of Materials Science and Engineering, Anyang Institute of Technology, Anyang 455000, China*

<sup>2</sup>*School of Foreign Languages, Anyang Institute of Technology, Anyang 455000, China*

<sup>3</sup>*State Key Laboratory for Mechanical Behavior of Materials, Xi'an Jiaotong University, Xi'an 710049, China*

received May 30, 2022; received in revised form November 24, 2022; accepted November 25, 2022

## Abstract

Low-sintering-temperature  $(\text{Na}_{1-x}\text{K}_x)_2\text{Mo}_2\text{O}_7$  ( $0.0 \leq x \leq 0.2$ ) ceramic was fabricated with the modified solid-phase sintering method. The sintering character and microwave dielectric property of the  $(\text{Na}_{1-x}\text{K}_x)_2\text{Mo}_2\text{O}_7$  ( $0.0 \leq x \leq 0.2$ ) ceramic were studied systematically. With the modified solid phase sintering method and ion substitution, the mass transfer efficiency of the ceramic powder was improved in the sintering procedure, which decreased the sintering temperature of the  $\text{Na}_2\text{Mo}_2\text{O}_7$  ceramic from 575 °C to 440 °C. Among the components, the  $(\text{Na}_{0.8}\text{K}_{0.2})_2\text{Mo}_2\text{O}_7$  ceramic was sintered well at 440 °C with a permittivity of 10.0, a  $Q \times f$  value of 48 000 GHz and a temperature coefficient of -75 ppm/K. The modified solid-phase sintering method is a potential substitution for the conventional solid-state method and the ion substitution is an effective way to further lower the sintering temperature.

*Keywords:* Low sintering temperature, sintering performance, dielectric ceramic

## I. Introduction

In 1901, the first radio wave communication experiment was conducted in a laboratory in England. Then, the first microwave communication circuit was established between England and France in 1955. Thanks to the breakthrough in microelectronic technology and digital processing technology, the microwave communication technology developed rapidly in 20th century. Of all the materials, low-temperature co-fired ceramic (LTCC) played a key role in the development of passive integration technology<sup>1</sup>, which is attributed to its excellent sintering and dielectric properties. Since the 21st century, the flexible wearable material has attracted the attention of many scientists and become a research hotspot. Owing to its low sintering temperature, the dielectric ceramic has the potential to be co-fired with organic material<sup>2</sup>. Materials prepared with this method exhibit both the dielectric property of the ceramic and the flexibility of the organic material. So, they can be used in medical and biological fields. However, compared with the melting point of the organic material, the sintering temperature of the existing ceramic is too high<sup>3</sup>, leading to a strong drive to decrease the sintering temperature of the ceramic<sup>4</sup>.

In general, adding sintering additive and solid solution are common ways to lower the sintering temperature of the ceramic. As established in our previous work<sup>5</sup>, the sintering additive cannot be completely burnt out. So, ethanol is chosen to replace polyvinyl ethanol (PVA) to wet the powder and isostatic pressing technology is applied in

preparation of the green ceramic body. Owing to the improvement in the solid-phase method, the adverse effect of the sintering additive is eliminated. As a result, the dielectric property of  $\text{K}_2\text{Mo}_2\text{O}_7$  ceramic, particularly the  $Q \times f$  value, is improved considerably. However, the effect of the modified solid-phase method on the sintering temperature has not been studied. The amelioration in preparation procedure may affect the mass transfer efficiency and lower the sintering temperature of the ceramic. Meanwhile, a number of experiments<sup>6-10</sup> has shown that suitable elemental doping changes the ion type in the crystal structure, which has an effect on the dielectric property. Moreover, the elemental doping changes the crystal lattice parameter and introduces point defects. So, it is estimated that the sintering property of the ceramic is affected.

In previous work<sup>11</sup>, the  $\text{Na}_2\text{Mo}_2\text{O}_7$  ceramic was prepared with traditional sintering method and has an excellent microwave dielectric property:  $\epsilon_r = 12.9$ ,  $Q \times f = 62\,400$ ,  $\text{TCF} = -72$  ppm/K and  $\text{S.T.} = 575$  °C. In order to reduce the sintering temperature of  $\text{Na}_2\text{Mo}_2\text{O}_7$  ceramic, the ceramic sample is prepared with the modified solid-reaction method in this work. Moreover,  $\text{K}^+$  and  $\text{Na}^+$  have the same valency and the ionic radius of  $\text{K}^+$  is larger than that of  $\text{Na}^+$  in the same coordination environment. The change of the ionic radius at A-site has the potential to change the crystal lattice parameter, which may improve the mass transfer efficiency in the sintering process and lower the sintering temperature. Thus, the partial substitution of  $\text{K}^+$  for  $\text{Na}^+$  is also completed. The result shows that the sintering property of the  $\text{Na}_2\text{Mo}_2\text{O}_7$  ceramic is much improved and the sintering temperature drops to 440 °C.

\* Corresponding author: [yxiaofeng@ayit.edu.cn](mailto:yxiaofeng@ayit.edu.cn)

## II. Experimental

Firstly, high-purity powders of  $\text{MoO}_3$  (> 99.5 %),  $\text{K}_2\text{CO}_3$  (> 99 %) and  $\text{Na}_2\text{CO}_3$  (99.8 %) were placed in the oven at 120 °C for 24 h to remove the moisture. The powders were then weighed and mixed according to the chemical molar ratio of  $(\text{Na}_{1-x}\text{K}_x)_2\text{Mo}_2\text{O}_7$ . Subsequently, the powder mixtures were transferred to agate jars and mechanically milled in a planetary mill (QM-3SP2; Nanjing Machine Factory, Nanjing, China) with  $\text{ZrO}_2$  balls at the speed of 150 rpm for 4 h. After being dried in the oven, the powder mixtures were loaded into crucibles and calcined at 400 °C for 6 h in air atmosphere. In order to reduce the particle size, the calcined powders were milled again for 4 h. After being dried, the powders were sprayed with moderate ethanol and pressed into cylindrical pellets (about 5 mm in thickness and 10 mm in diameter) under 150 MPa uniaxial stress. Subsequently, all the cylindrical samples were pressed again in an isostatic press (CIP AIP3-12-60C, American Isostatic Presses, Columbus, America) at the pressure of 200 MPa for 3 min. Finally, the samples were held at 120 °C for 2 h to remove the ethanol and then sintered at 420–500 °C for 6 h at the heating rate of 2 K/min.

The phase composition of the sample was analysed with powder X-ray diffraction (XRD). The microstructure was observed with scanning electron microscopy (SEM). The average grain size was measured with the linear intercept method, which complied with the BS EN 623-3:2001 standard. The sintering properties were measured on a

high-precision electronic balance with the Archimedes method. Dielectric properties of the prepared sample were measured with a network analyzer and in a temperature chamber with the TE01 $\delta$  shielded cavity method at room temperature. The relationship between the resonant frequency and temperature ( $\tau_f$ ) was calculated according to the following formula:

$$\tau_f = (f_{85} - f_{25}) / f_{25} (85 - 25) \times 10^6 \text{ (ppm/K)} \quad (1)$$

where  $f_{85}$  and  $f_{25}$  were the measured resonant frequencies at 85 °C and 25 °C, respectively.

## III. Result and Discussion

Fig. 1(a) shows the XRD result of the  $(\text{Na}_{1-x}\text{K}_x)_2\text{Mo}_2\text{O}_7$  ceramic calcined at 400 °C and Fig. 1(b) shows the enlarged drawing of XRD results between 22° and 26°. It is found from Fig. 1(a) that when  $x = 0.0$ , pure  $\text{Na}_2\text{Mo}_2\text{O}_7$  ceramic was obtained. Based on comparison with the PDF card 22-0906, the  $\text{Na}_2\text{Mo}_2\text{O}_7$  ceramic belongs to orthorhombic phase structure, which agrees well with the previous work<sup>11</sup>. Meanwhile, no secondary phase is found when  $x \leq 0.2$ . It indicates that the substitution of  $\text{K}^+$  for  $\text{Na}^+$  is achieved and has a slight influence on the  $\text{Na}_2\text{Mo}_2\text{O}_7$  crystal structure at low doping level. Moreover, it can be clearly observed from Fig. 1(b) that the reflection peak, such as (023), moves to left with the increase of  $\text{K}^+$  doping level. Theoretically, the relation between the position of the characteristic reflection peak and the lattice parameter can be analysed based on Bragg's law.

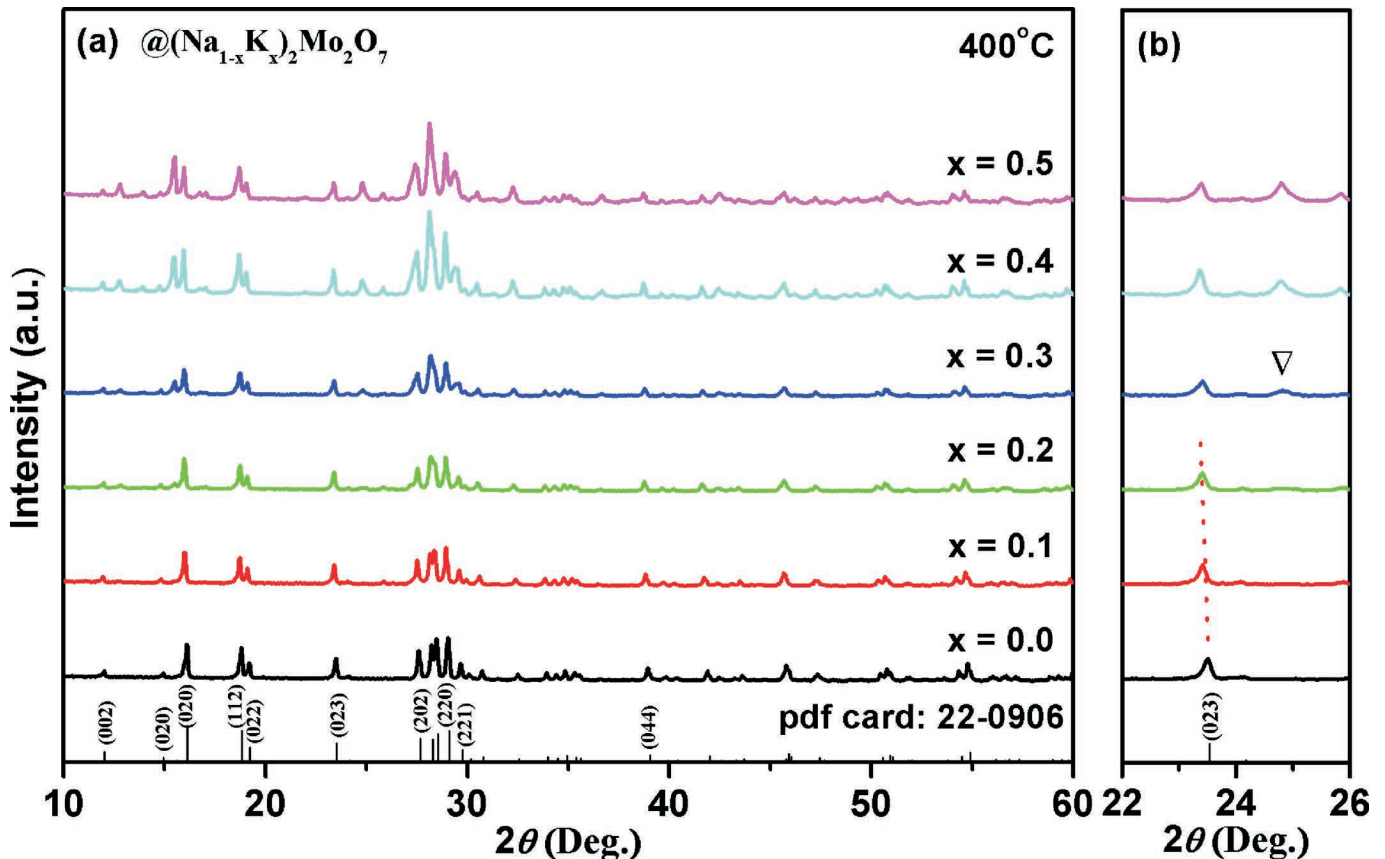


Fig. 1: XRD patterns of the  $(\text{Na}_{1-x}\text{K}_x)_2\text{Mo}_2\text{O}_7$  ceramic calcined at 400 °C.

$$2d \sin\theta = n\lambda \quad (2)$$

where  $d$  is the distance of adjacent crystal faces,  $\theta$  is the scattering angle of the machine,  $n$  is a positive integer and  $\lambda$  is the wavelength of the incident wave. In the same coordination environment, the ionic radius of  $\text{K}^+$  is larger than that of  $\text{Na}^+$  <sup>12-13</sup>. Owing to the change of the ionic radius at A-site, the characteristic reflection peak moves to the left. However, the characteristic reflection peak of the impurity appears when  $x = 0.3$ , which means the  $(\text{Na}_{1-x}\text{K}_x)_2\text{Mo}_2\text{O}_7$  ceramic belongs to limited solid solution system. With the increase in the doping level, the difference between  $\text{K}^+$  and  $\text{Na}^+$  introduces more stress into the crystal structure, which leads to the destruction of the structure. As a result, the impurity phase appears.

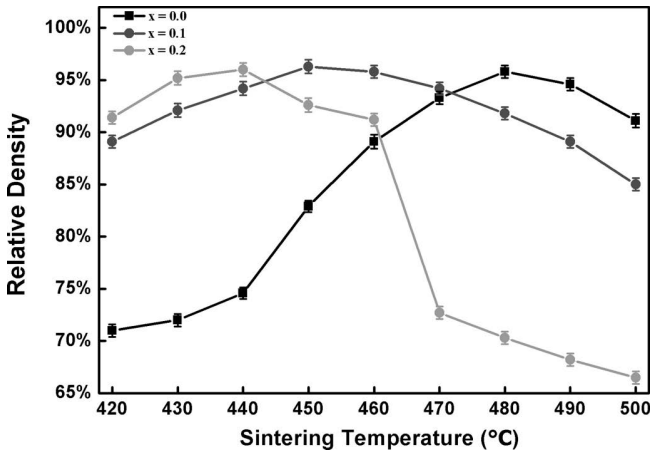


Fig. 2: Relative densities of the  $(\text{Na}_{1-x}\text{K}_x)_2\text{Mo}_2\text{O}_7$  ceramic sintered at different temperature.

Fig. 2 shows the relative density of all the samples sintered at different temperature. Considering the water-soluble property of molybdate system, all the samples were placed in the oven at 120 °C for 4 h before being measured with the Archimedes method. It can be observed from Fig. 2 that, due to the grain growth and the decrease of porosity, the relative density increases with the sintering temperature in the initial sintering stage. Finally, the  $(\text{Na}_{1-x}\text{K}_x)_2\text{Mo}_2\text{O}_7$  ceramic is sintered well at 480 °C (95.8 %) for  $x = 0.0$ , 450 °C (96.3 %) for  $x = 0.1$  and 440 °C (96.1 %) for  $x = 0.2$ . The relative density of all the components is very high, which means the ceramic sample is

dense. However, as the sintering temperature continues to rise, the density of the sample drops sharply.

Fig. 3 presents the SEM images of the sintered  $(\text{Na}_{1-x}\text{K}_x)_2\text{Mo}_2\text{O}_7$  ceramic sample. For all the samples, the grains are compact and can be observed clearly. Owing to the improvement in preparation, the impact of the sintering additive is totally eliminated and the mass transfer efficiency during the sintering process is improved. So, the grain boundary in this work is much clearer and the grain grows sufficiently. The average grain size is measured as 3.42  $\mu\text{m}$  for  $x = 0.0$ , 1.86 for  $x = 0.1$  and 1.72 for  $x = 0.2$ . As shown in Fig. 3(b-c), the  $\text{K}^+$  doping has an impact on the grain size and shape. The average grain size decreases with  $x$  value. Conventionally, ion substitution will introduce point defects in the sample <sup>14-17</sup>. The introduced point defects slow the movement of the grain boundary, which prevents the further growth of the grain.

#### IV. Conclusions

Fig. 4 shows the SEM result for the  $x = 0.2$  sample sintered at different temperatures. With the increase of the sintering temperature, the grain grows abnormally <sup>18-23</sup>. The secondary growth of the grain destroys the grain boundary and introduces pores into the ceramic sample. So, the relative density of the sample declines if the sintering temperature exceeds the optimum value.

Fig. 5 presents the microwave dielectric properties of  $(\text{Na}_{1-x}\text{K}_x)_2\text{Mo}_2\text{O}_7$  ceramic. As shown in Fig. 5, the  $x = 0.0$  sample can be sintered well at 480 °C with a permittivity of 12.6, a  $Q \times f$  value of 59 100 GHz and a TCF value of -77 ppm/K in this work. The  $x = 0.1$  sample possesses the excellent property with sintering temperature of 450 °C, a permittivity of 12.0, a  $Q \times f$  value of 48 630 GHz and a TCF value of -75 ppm/K. After the doping level is further increased, the  $x = 0.2$  sample can be sintered well at 440 °C for 6 h with a permittivity of 10.0, a  $Q \times f$  value of 48 000 GHz and a TCF value of -75 ppm/K. Compared with the research on  $\text{Na}_2\text{Mo}_2\text{O}_7$  ceramic in our previous work <sup>11</sup>, the sintering temperature decreases from 575 °C to 480 °C. It means that the modified solid-phase sintering method can reduce the sintering temperature effectively. The sintering process of the ceramic is in essence a mass transfer process. The particles in the sample rearrange in the initial sintering stage and the pores become smaller, which results in

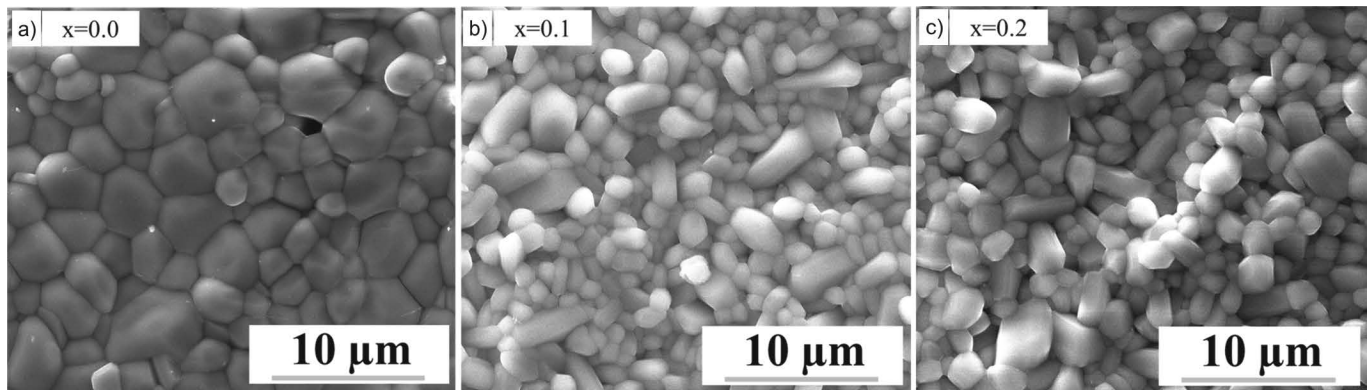


Fig. 3: Scanning electron microscopy photos of  $x = 0.0$  sintered at 480 °C,  $x = 0.1$  sintered at 450 °C and  $x = 0.2$  sintered at 440 °C.



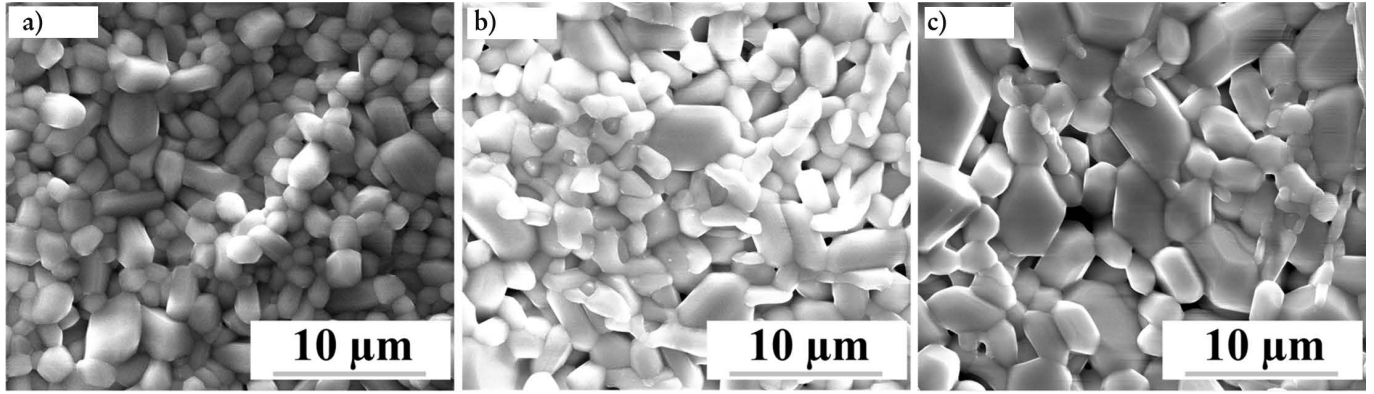


Fig. 4: Scanning electron microscopy images of  $x = 0.2$  sintered at 440 °C, 450 °C and 460 °C.

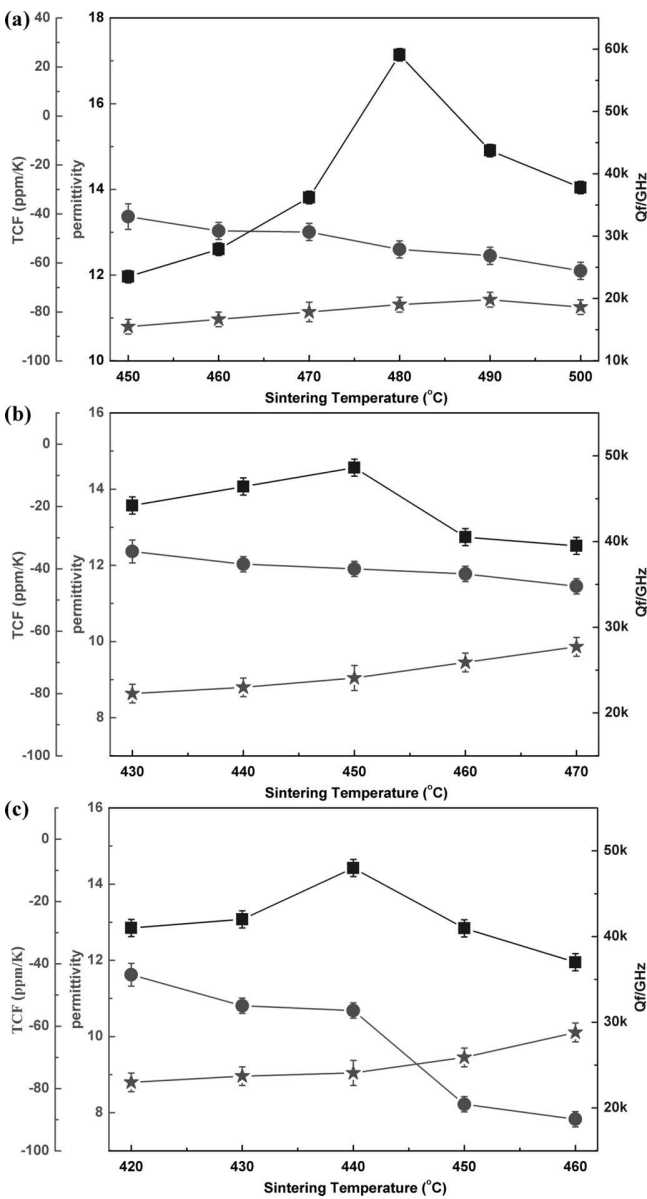


Fig. 5: Microwave dielectric properties (■:  $Q \times f$  value, ●: permittivity, ★: TCF value) of (a)  $x = 0.0$ , (b)  $x = 0.1$  and (c)  $x = 0.2$  as a function of the sintering temperature.

the reduction of porosity and the contact between the particles<sup>24–26</sup>. Subsequently, the material diffusion process begins between the particles. Obviously, the boundary is

not currently straight. Then, stress builds up between the adjacent grains:

$$\Delta p = (1/r_1 + 1/r_2)\gamma \quad (3)$$

Where  $r_1$  and  $r_2$  are curvature radii of the adjacent grains,  $\gamma$  is the magnitude of the surface tension.

Being driven by the pressure, the powders begin to spread through holes and defects, which leads to the movement of the grain boundary and the growth of the grain. As a result, the large pores and small grains disappear. The density of the sample increases in this process. Finally, the ceramic sample gradually becomes compact during the sintering process. As one kind of organic material, the residual PVA prevents the movement of the powder and reduces the mass transfer efficiency. As a result of the improved preparation process, the sintering temperature decreases a lot, which is due to the improvement in the density and no organic residue in the sample. Meanwhile, it is found from Fig. 5 (b-c) that the sintering temperature drops from 480 °C for  $x = 0.0$  to 440 °C for  $x = 0.2$ . Many studies<sup>27–28</sup> show that the ion substitution changes the lattice parameter and introduces point defects into the ceramic sample. The introduced point defect becomes an ion-diffusion channel, which improves the mass transfer efficiency<sup>29–30</sup>. As a result, the  $x = 0.2$  sample can be sintered well at lower temperature.

The solid-solution  $(Na_{1-x}K_x)_2Mo_2O_7$  ( $0.0 \leq x \leq 0.2$ ) ceramic was synthesized and systematically studied in this work. The sintering temperature of the pure  $Na_2Mo_2O_7$  ceramic drops from 575 °C to 480 °C, which is ascribed to the amelioration in the solid-state reaction method. Subsequently, the  $Na^+$  is partly substituted by  $K^+$  and the XRD result indicates that the substitution is achieved. Owing to the ion doping, the sintering temperature further drops to 440 °C for  $x = 0.2$ . After being sintered at 440 °C for 6 h, the  $x = 0.2$  possesses the best property with a permittivity of 10.0, a  $Q \times f$  value of 48 000 GHz and a TCF value of -75 ppm/K. It is found that using isostatic pressing technology and ethanol can improve the mass transfer efficiency during the sintering process, which reduces the sintering temperature of the ceramic. Besides, ionic solid solution is an effective method to further lower the sintering temperature.

## Acknowledgements

This work is supported by the Doctoral Foundation of Anyang Institute of Technology (Grant No. BSJ 2021010), Scientific and technological project of Henan Province (Grant No. 2221022230020).

## References

- Sebastian, M.T., Jantunen, H.: Low-loss dielectric materials for LTCC applications: a review, *Int. Mater. Rev.*, **53**, 57–90, (2008).
- Sebastian, M.T., Ubic, R., Jantunen, H.: Low-loss dielectric ceramic materials and their properties, *Int. Mater. Rev.*, **60**, 392–412, (2015).
- Sebastian, M.T., Wang, H., Jantunen, H.: Low temperature co-fired ceramics with ultra-low sintering temperature: a review, *Curr. Opin. Solid State Mater. Sci.*, **20**, 151–170, (2016).
- Braginsky, V.B., Ilschenko, V.S., Bagdassarov, K.S.: Experimental observation of fundamental microwave absorption in high quality dielectric crystals, *Appl. Phys. A*, **120**, 300–305, (1987).
- Yuan, X.F., Zhang, G.Q., Wang, H.: A novel solid solution  $(\text{K}_{1-x}\text{Na}_x)_2\text{Mo}_2\text{O}_7$  ( $0.0 \leq x \leq 0.3$ ) ceramics with ultralow sintering temperatures, *J. Eur. Ceram. Soc.*, **38**, 4967–4971, (2018).
- Valant, M., Suvorov, D.: Processing and dielectric properties of sillenite compounds  $\text{Bi}_{12}\text{MO}_{20-\delta}$  ( $\text{M} = \text{Si}, \text{Ge}, \text{Ti}, \text{Pb}, \text{Mn}, \text{B}_{1/2}\text{P}_{1/2}$ ), *J. Am. Ceram. Soc.*, **84**, 2900–2904, (2001).
- Zhang, P., Liu, J., Zhao, Y.: Effects of MgO-LiF addition on the sintering behavior and microwave dielectric properties of  $\text{Li}_2\text{MgTi}_3\text{O}_8$  ceramics, *Mater. Lett.*, **162**, 173–175, (2016).
- Lin, H., Yang, A., Luo, L.: Microwave dielectric properties of low temperature co-fired glass-ceramic based on  $\text{B}_2\text{O}_3$ - $\text{La}_2\text{O}_3$ -MgO glass with  $\text{La}(\text{Mg}_{0.5}\text{Ti}_{0.5})\text{O}_3$  ceramics, *Mater. Lett.*, **62**, 611–614, (2008).
- Huang, C.L., Yang, W.R.: Effect of CuO addition to  $\text{Nd}(\text{Zn}_{1/2}\text{Ti}_{1/2})\text{O}_3$  ceramics on sintering behavior and microwave dielectric properties, *Mater. Lett.*, **63**, 103–105, (2009).
- Wang, S.H., Zhou, H.P., Chen, K.X., et al.: Sintering and properties of  $\text{CaO-Al}_2\text{O}_3\text{-B}_2\text{O}_3\text{-SiO}_2$  system glass ceramics, *Key Eng. Mater.*, **247**, 389–392, (2003).
- Zhang, G.Q., Guo, J., He, L., et al.: Ultra-low sintering temperature microwave dielectric ceramics based on  $\text{Na}_2\text{O-MoO}_3$  binary system, *J. Am. Ceram. Soc.*, **98**, 528–533, (2015).
- Shannon, R.D.: Dielectric polarizabilities of ions in oxides and fluorides, *J. Appl. Phys.*, **73**, 348–366, (1993).
- Kim, K.S., Sang, H.S., Kim, S., et al.: Microwave dielectric properties of ceramic/glass composites with bismuth-zinc borosilicate glass, *J. Ceram. Process. Res.*, **11**, 47–51, (2010).
- Zhou, D., Rall, C.A., Wang, H., et al.: Ultra-low firing high-k scheelite structures based on  $[(\text{Li}_{0.5}\text{Bi}_{0.5})_x\text{Bi}_{1-x}][\text{Mo}_x\text{V}_{1-x}]\text{O}_4$  microwave dielectric ceramics, *J. Am. Ceram. Soc.*, **93**, 2147–2150, (2010).
- Zhou, D., Pang, L.X., Guo, J., et al.: Phase evolution, phase transition, Raman spectra, infrared spectra, and microwave dielectric properties of low temperature firing  $(\text{K}_{0.5x}\text{Bi}_{1-0.5x})(\text{Mo}_x\text{V}_{1-x})\text{O}_4$  ceramics with scheelite related structure, *Inorg. Chem.*, **50**, 12733–12738, (2011).
- Wang, S.F., Wang, Y.R., Hsu, Y.F., et al.: Ultra-low-fire  $\text{Te}_2(\text{Mo}_{1-x}\text{W}_x)\text{O}_7$  ceramics: microstructure and microwave dielectric properties, *J. Am. Ceram. Soc.*, **93**, 4071–4074, (2010).
- Zhou, D., Pang, L.X., Xie, H.D., et al.: Crystal structure and microwave dielectric properties of an ultralow-temperature-fired  $(\text{AgBi})_{0.5}\text{WO}_4$  ceramic, *Eur. J. Inorg. Chem.*, **2014**, 296–301, (2014).
- Kwon, D.K., Lanagan, M.T., Shrout, T.R.: Microwave dielectric properties of  $\text{BaO-TeO}_2$  binary compounds, *Mater. Lett.*, **61**, 1827–1831, (2007).
- Subodh, G., Ratheesh, R., Jacob, M.V., et al.: Microwave dielectric properties and vibrational spectroscopic analysis of  $\text{MgTe}_2\text{O}_5$  ceramics, *J. Mater. Res.*, **23**, 1551–1556, (2008).
- Udovic, M., Valant, M., Suvorov, D.: Phase formation and dielectric characterization of the  $\text{Bi}_2\text{O}_3\text{-TeO}_2$  system prepared in an oxygen atmosphere, *J. Am. Ceram. Soc.*, **87**, 591–597, (2004).
- Valant, M., Suvorov, D.: Glass-free low-temperature cofired ceramics: calcium germanates, silicates and tellurates, *J. Eur. Ceram. Soc.*, **24**, 1715–1719, (2004).
- Wang, S.F., Hsu, Y.F., Wang, Y.R., et al.: Ultra-low-fire  $\text{Zn}_2\text{Te}_3\text{O}_8\text{-TiTe}_3\text{O}_8$  ceramic composites, *J. Am. Ceram. Soc.*, **94**, 812–816, (2011).
- Subodh, G., Sebastian, M.T.: Glass-free  $\text{Zn}_2\text{Te}_3\text{O}_8$  microwave ceramic for LTCC applications, *J. Am. Ceram. Soc.*, **90**, 2266–2268, (2007).
- Chang, L.Y., Sachdev, S.: Alkali tungstates: stability relations in the systems  $\text{A}_2\text{O-WO}_3\text{-WO}_3$ , *J. Am. Ceram. Soc.*, **58**, 267, (1975).
- Okada, K., Morikawa, H., Marumo, F.: Sodium tungstate, *Acta Crystallogr. Sect.*, 1974, **B30**, (1872).
- Mendelson, M.I.: Average grain size in polycrystalline ceramics, *J. Am. Ceram. Soc.*, **52**, 443–446, (1969).
- Guo, M., Gong, S.P., Dou, G., et al.: A new temperature stable microwave dielectric ceramics:  $\text{ZnTiNb}_2\text{O}_8$  sintered at low temperatures, *J. Alloy. Compd.*, **509**, 5988–5995, (2011).
- Wu, Y., Zhou, D., Guo, J., et al.: Temperature stable microwave dielectric ceramic  $0.3\text{Li}_2\text{TiO}_3\text{-}0.7\text{Li}(\text{Zn}_{0.5}\text{Ti}_{1.5})\text{O}_4$  with ultra-low dielectric loss, *Mater. Lett.*, **65**, 2680–2682, (2011).
- Penn, S.J., Alford, N., Templeton, A., et al.: Effect of porosity and grain size on the microwave dielectric properties of sintered alumina, *J. Am. Ceram. Soc.*, **80**, 1885–1888, (1997).
- Alford, N.M., Breeze, J., Wang, X., et al.: Dielectric loss of oxide single crystals and polycrystalline analogues from 10 to 320 K, *J. Eur. Ceram. Soc.*, **21**, 2605–2611, (2001).

